Counting defects in an instantaneous quench

D. Ibaceta* and E. Calzetta†
Department of Physics and Instituto de Astronomia y Física del Espacio, University of Buenos Aires, Buenos Aires, Argentina
(Received 9 October 1998)

We consider the formation of defects in a nonequilibrium second-order phase transition induced by an instantaneous quench to zero temperature in a type II superconductor. We perform a full nonlinear simulation where we follow the evolution in time of the local order parameter field. We determine how far into the phase transition theoretical estimates of the defect density based on the Gaussian approximation yield a reliable prediction for the actual density. We also characterize quantitatively some aspects of the out of equilibrium phase transition. [S1063-651X(99)09408-8]

PACS number(s): 05.70.Fh, 11.27.+d, 11.10.Wx, 67.40.Vs

I. INTRODUCTION

The objective of this paper is to study the formation of defects in a nonequilibrium second-order phase transition by means of a numerical solution of the full dynamical equations, and to compare the results with theoretical predictions to be found in the literature [1–3]. Topological defects are a common occurrence in symmetry broken field theories [4], with far reaching consequences in condensed matter physics [5], particle physics [6,7], and cosmology [8]. The equilibrium structure of defects is deeply rooted in the topological aspects of the theory, and is well understood. The dynamical formation of defects in the process of a nonequilibrium phase transition, on the other hand, only recently has been the subject of a systematic analysis.

The issue at stake is how many defects are to be formed as a function of both the dynamics of the system and the macroscopic parameters characterizing the transition, such as cooling rates. A simple, order of magnitude, estimate is based on the observation that once the system is cold enough, defects will be unable either to form or disappear through thermal activation, so they will be essentially frozen into existence. This happens at the so-called Ginzburg temperature, and leads to the prediction that the typical distance between defects is of the order of magnitude of the correlation length at this temperature [9].

This picture of defect dynamics has been criticized by Zurek and co-workers as downplaying the nonequilibrium features of the process [10,11]. According to these authors, the freezing of defects occurs at a much higher temperature, when the relaxation time of the system becomes large and the system effectively decouples from its environment. Their arguments usually lead to higher defect densities than found previously, a prediction confirmed by some experiments [12,13] (see, however, Ref. [14]). They are also supported by numerical simulations in one- and two-dimensional Ginzburg-Landau systems with broken global symmetries [15].

Complementary to the search for a qualitative understanding of defect formation, some authors have attempted to derive the density of defects from a first-principles description of the dynamics. As a matter of fact, there is a rigorous result linking the density of defects to the equal time correlation function for the order parameter, valid whenever the field probability distribution is Gaussian [1,2]. Under the Gaussian approximation, then, finding the density of defects is reduced to solving the dynamics for the correlation function [3]. This approach, which has recently been used to show the validity of Zurek and co-workers estimates in a quantum field theoretic model [16], is usually though to be correct early in the development of the phase transition [17].

In order to evaluate how reliable this kind of argument really is, therefore, we must know how far in the phase transition the Gaussian approximation may be trusted. Since the development of the phase transition is an essentially nonlinear process, we must expect that non-Gaussian correlations will be created by the dynamics itself, even if suppressed in the initial conditions. There will be a competition between the characteristic growth time due to the spinodal instability [18,19], and a variety of dynamical times describing the building of correlations through nonlinear interaction of fluctuations; however, the usual Gaussian models do not give us a clue about what the latter might be.

The objective of this paper is to give a tentative answer to the question of the reliability of defect density estimates based on the Gaussian approximation, by presenting a fully nonlinear simulation of a phase transition where we have measured the Gaussianity of the order parameter, the Gaussian prediction for the density of defects, and the actual density, as functions of time. Of course, as long as the field is actually Gaussian, the rigorous analytic prediction for the defect density is validated. The nontrivial issue is how long the field probability density remains Gaussian, and whether the Gaussian prediction continues to hold beyond that point. Concretely, we find that even when Gaussianity of the ensemble ceases to hold, the prediction remains valid, to break down about the time defects are definitely formed.

Our simulations follow the unfolding of an instantaneous quench to zero temperature in a two-dimensional type-II superconductor, described by the time-dependent Landau-Ginzburg equations derived by Gor'kov and Eliashberg [20] (see also Refs. [21–24]). This model is a scalar field theory interacting with a U(1) gauge field (see Ref. [11]), but with the presence of a normal current, in addition to the supercurrent, and a first order (rather than second one) equation for the vector potential **A** (see below).

In order to perform the simulations, we have discretized the model and placed it on a square lattice, with periodic

*Electronic address: ivan@df.uba.ar
†Electronic address: calzetta@df.uba.ar

boundary conditions. Our discrete model still has gauge symmetry, which is preserved by the evolution. We have further considered a variety of lattice sizes and initial conditions, thus making sure that our results truly reflect the physics of the system. We have identified defects by measuring the winding number of the field around each lattice plaquette, thus avoiding the uncertainties related to identifying defects from zeros in the order parameter [25].

We find that the evolution of a typical quench goes through three well defined regimes. The early development is dominated by the exponential growth of the order parameter; the different modes of the field evolve independently, and the field remains Gaussian. In this regime, the Halperin-Mazenko-Liu (HML) prediction for the defect density is very accurate. This regime ends when the order parameter reaches about a tenth of its equilibrium value.

The second regime is a transitional epoch dominated by the actual formation of the defects. During this transitional epoch, the field departs from Gaussianity in a significant way, but the HML prediction is still a good approximation to the actual density. Finally, in the late time regime both the Gaussian approximation for the order parameter and the HML prediction are unreliable.

We may therefore conclude that, as argued by Karra and Rivers [3], the HML prediction holds early in the development of the phase transition, being a very accurate estimate of the actual density until the time the defects may be considered as definitely formed, which is also the time when the order parameter reaches about half of its equilibrium value. It is therefore a suitable means to estimate the initial conditions for the subsequent evolution of the defect network, as determined by defect-defect interactions and changes in the environment, such as the expansion of the Universe in cosmological applications [8]. Our results validate previous analyses of nonequilibrium defect formation, such as Refs. [1–3,16].

The paper is organized as follows. Section II introduces the theoretical prediction of the defect density for a Gaussian quench. Section III shows the time-dependent Ginzburg-Landau model, and the numerical details related to its implementation. Section IV describes the resulting quenches and the conclusions, and the paper ends with some final remarks.

II. THEORETICAL PREDICTION

At a qualitative level, the formation of topological defects is well understood through the symmetry breaking mechanism. For a complex scalar field, the true ground-state manifold of the field is $S1$, and the phase of the field at different points can be different. If eventually the winding number of the field along a closed loop is not zero, then topological defects are trapped inside. Because of topological considerations, isolated defects at low temperature are stable, although defects may interact with each other and annihilate, migrate to the boundaries of the system, or, in cosmology, decay through gravitational radiation.

We are searching for the monopoles of one complex order parameter field Φ in two dimensions. This will be identified with the zeros of the field with a nontrivial winding number. If they are located at $\mathbf{x}_1,\mathbf{x}_2,\mathbf{x}_3,\ldots$, we obtain for the total and topological densities

$$\overline{\rho}(\mathbf{x})=\sum_i \delta(\mathbf{x}-\mathbf{x}_i),$$
$$\rho(\mathbf{x})=\sum_i n_i\delta(\mathbf{x}-\mathbf{x}_i), \tag{1}$$

where n_i is the winding number of each defect, i.e., its topological charge.

The total density of defects is obtained through the relation between zeros of the field and the field itself, i.e., the Jacobian [3]

$$\overline{n}(t)=\langle\overline{\rho}(\mathbf{x})\rangle=\int \mathcal{D}\Phi p_t[\Phi]\delta^2[\Phi]|\epsilon_{jk}\partial_j\Phi_1(\mathbf{x})\partial_k\Phi_2(\mathbf{x})|, \tag{2}$$

with $\epsilon_{12}=-\epsilon_{21}=1$ (otherwise zero) and $\Phi=(\Phi_1+i\Phi_2)/\sqrt{2}$, p_t being the probability density of the different field configurations.

For the Gaussian model we have $\langle\Phi_a(\mathbf{x})\rangle=0=\langle\Phi_a(\mathbf{x})\partial_j\Phi_b(\mathbf{x})\rangle$. Assuming also that the equal-time Wightman function $\langle\Phi_a(\mathbf{x})\Phi_b(\mathbf{y})\rangle=W_{ab}(|\mathbf{x}-\mathbf{y}|;t)=\delta_{ab}W(|\mathbf{x}-\mathbf{y}|;t)$ is the only nonvanishing correlation function and is diagonal, then [1,2]

$$\overline{n}(t)=\frac{1}{2\pi}(-f''(0;t)), \tag{3}$$

where

$$f(r;t)=\frac{W(r;t)}{W(0;t)}, \tag{4}$$

and derivatives are taken with respect to r.

To compute the right-hand side of Eq. (3), we consider the Fourier transform of the field, $\tilde{\Phi}(\mathbf{k})=\int d\mathbf{x}\exp(i\mathbf{k}\cdot\mathbf{x})\Phi(\mathbf{x})$, in order to obtain

$$f''(0;t)=-\frac{\int d\mathbf{k}\,k^2|\tilde{\Phi}(\mathbf{k})|^2}{\int d\mathbf{k}|\tilde{\Phi}(\mathbf{k})|^2}. \tag{5}$$

Our goal is to test the range of validity of the relation (3) by measuring both sides of this equation independently.

III. MODEL

A. Theory

The time-dependent Ginzburg-Landau equation describes the time-space dependence of the order parameter of a superconductor [20]. Normalized in the form adopted by Hu and Thompson, it reads [21–23]

$$\frac{1}{D}\left[\frac{\partial}{\partial t}+i\frac{2e}{\hbar}\psi\right]\Delta+\xi(T)^{-2}(|\Delta|^2-1)\Delta+\left[\frac{\nabla}{i}-\frac{2e}{\hbar c}\mathbf{A}\right]^2\Delta-f(\mathbf{r},t)=0, \tag{6}$$

where

$$\mathbf{j}=\sigma\left[-\nabla\psi-\frac{1}{c}\frac{\partial\mathbf{A}}{\partial t}\right]+\mathrm{Re}\left[\Delta^*\left[\frac{\nabla}{i}-\frac{2e}{\hbar c}\mathbf{A}\right]\Delta\right]\frac{\hbar c^2}{8\pi e\lambda(T)^2}, \tag{7}$$

$$\rho=\frac{\psi-\varphi}{4\pi\lambda_{TF}^2}. \tag{8}$$

With the Maxwell equations coupling the electromagnetic potentials to charge and current densities, they provide a full set of evolution equations. Here D is the normal-state diffusion constant, σ is the normal-state conductivity given by $\sigma=(c^2\xi^2/48\pi\lambda^2)(1/D)$, and ρ and j are the charge and current densities. f is a finite temperature random driving force; since we shall consider a quench to zero temperature, it will eventually be set to zero (see below). Furthermore, the order parameter is divided by its equilibrium value $\Delta_\infty=\pi k\sqrt{2(T_c^2-T^2)}$, where T_c is the critical temperature. Note that this is a temperature-dependent parametrization.

$\mathbf{A}$ and φ are the vector and scalar potentials, respectively, and ψ is the electrochemical potential divided by the electronic charge. Assuming $\rho=0$ (that is, absence of net charge at the grid scale), results in $\psi=\varphi$ (see Refs. [20,21]).

This set of equations is invariant under the gauge transformation:

$$\begin{aligned}\mathbf{A}&\rightarrow\mathbf{A}-\nabla\chi,\\ \varphi&\rightarrow\varphi+\frac{1}{c}\frac{\partial\chi}{\partial t},\\ \Delta&\rightarrow\Delta\exp\left[-i\frac{2e}{\hbar c}\chi\right].\end{aligned} \tag{9}$$

From the microscopic theory, we have the relationships

$$\frac{4\pi\lambda(T)^2\sigma}{c^2}=\frac{\xi(T)^2}{12D}=\frac{\pi\hbar}{96k_BT_c}\left(1-\frac{T}{T_c}\right)^{-1}\equiv\frac{t_{GL0}}{12}\left(1-\frac{T}{T_c}\right)^{-1}, \tag{10}$$

where $\xi(T)=\xi(0)[1-(T/T_c)]^{-1/2}$ and $\lambda(T)=\lambda(0)[1-(T/T_c)]^{-1/2}$ are the temperature-dependent correlation (coherence) length and magnetic penetration depth, respectively, and $t_{GL0}=\pi\hbar/8k_BT_c$ is the characteristic relaxation time of the uniform mode at zero temperature.

We can write our model in terms of dimensionless variables as follows [24]:

$$\begin{aligned}t&\rightarrow tt_0\ \text{ with }\ t_0=\frac{\pi\hbar}{96k_BT_c}=\frac{t_{GL0}}{12},\\ r&\rightarrow r\xi(0),\\ A&\rightarrow A\frac{\Phi_0}{2\pi\xi(0)}\quad\text{with}\ \ \Phi_0=\frac{hc}{2e},\\ \varphi&\rightarrow\varphi\frac{\Phi_0}{2\pi ct_0},\\ j&\rightarrow j\frac{c\Phi_0}{8\pi^2\xi(0)},\\ f&\rightarrow f\xi(0)^2,\\ T&\rightarrow TT_c\end{aligned} \tag{11}$$

to obtain [20–23]

$$\begin{aligned}\frac{\partial}{\partial t}\Delta+i\varphi\Delta&=-\frac{1}{12}[(i\nabla+\mathbf{A})^2\Delta+(1-T)(|\Delta|^2-1)\Delta-f],\\ \frac{\partial}{\partial t}\mathbf{A}+\nabla\varphi&=(1-T)\mathrm{Re}[\Delta^*(-i\nabla-\mathbf{A})\Delta]-\kappa^2\nabla\times(\nabla\times\mathbf{A}),\end{aligned} \tag{12}$$

where $\kappa=\lambda(T)/\xi(T)$ is the temperature-independent Ginzburg-Landau (GL) parameter which characterizes the superconductor. For a type-II superconductor we have $\kappa>1/\sqrt{2}$. We have chosen $\kappa=\sqrt{2}$. The gauge freedom allows us to choose $\varphi\equiv0$.

Since we are interested in instantaneous quenches toward zero temperature, we set $T=0$ and $f=0$ [26]. Furthermore, we must prepare the system in some thermal equilibrium configuration. This means generating a set of initial conditions corresponding to a thermal distribution of modes [21],

$$\begin{aligned}\langle\tilde{\Delta}(\mathbf{k})\rangle&=0,\\ \langle\tilde{\Delta}(\mathbf{k})\tilde{\Delta}(\mathbf{0})\rangle&=\frac{1}{V}\frac{2m^*}{\hbar^2}\frac{k_BT}{k^2+1/\xi(T)^2},\end{aligned} \tag{13}$$

with a cutoff when $k\approx\xi_0^{-1}$ beyond which GL theory is not valid. Here $m^*=2m_e$ is the mass of the coupled electrons. In terms of dimensionless variables,

$$\langle|\tilde{\Delta}(\mathbf{k})|^2\rangle=\frac{\mu}{V}\frac{T}{k^2+\xi^{-2}}\quad\text{with}\ \mu=\frac{2k_BT_cm^*\xi(0)}{\hbar^2}. \tag{14}$$

The factor μ is clearly substance dependent and will be chosen later on.

B. Implementation

The discrete version of the gauge transformation is obtained through

$$\begin{aligned}A_\mu^j&\rightarrow A_\mu^j-\frac{(\chi^{j+\mu}-\chi^j)}{a_\mu},\\ \Delta^j&\rightarrow\Delta^j\exp[-i\chi^j],\end{aligned} \tag{15}$$

where μ stands for a direction and j for a site in the lattice. In order to obtain a discrete version of Eq. (12), invariant under Eq. (15), we employ the usual link variables technique from lattice QCD [7] as in Ref. [24]:

$$U_\mu^{r_1 r_2} = \exp\left[-i \int_{r_1}^{r_2} A_\mu d\mu \right] \rightarrow \text{discretized } U_\mu^{j,j+\mu} = \exp[-iA_\mu^j a_\mu]. \tag{16}$$

The differential operators become

$$\left[\frac{1}{i} \frac{\partial}{\partial x_\mu} - A_\mu \right] \Delta \rightarrow -i \frac{U_\mu^{j+\mu,j} \Delta^{j+\mu} - \Delta^j}{a_\mu}, \tag{17}$$

$$\left[\frac{1}{i} \frac{\partial}{\partial x_\mu} - A_\mu \right]^2 \Delta \rightarrow \frac{U_\mu^{j+\mu,j} \Delta^{j+\mu} - 2\Delta^j + U_\mu^{j-\mu,j} \Delta^{j-\mu}}{a_\mu^2}, \tag{18}$$

and the finite difference equations to solve are ($\Delta^j = \rho^j e^{i\theta^j}$)

$$\mathrm{Re}\,\dot{\Delta}^j = \frac{1}{12} \Bigg[(\rho^{j+x} \cos(-A_x^j a_x + \theta^{j+x}) - 2\,\mathrm{Re}\,\Delta^j + \rho^{j-x} \cos(A_x^{j-x} a_x + \theta^{j-x})) \frac{1}{a_x^2} + \cdots - (1-T) \times (\rho^{j2} - 1)\mathrm{Re}\,\Delta^j \Bigg] \tag{19}$$

for the real part of the order parameter field, and

$$\dot{A}_x^j = (1-T)\rho^j \rho^{j+x} \sin(-a_x A_x^j - \theta^j + \theta^{j+x}) \frac{1}{a_x} - \kappa^2 \left[\frac{A_y^{j+x+y} - A_y^{j+y} - A_y^{j+x} + A_y^j}{a_x a_y} - \frac{A_x^{j+y} - 2A_x^j + A_x^{j-y}}{a_y a_y} \right] \tag{20}$$

for the x component of the gauge field. We choose here to work directly with the fields, but alternatively link variables can be used [24].

We evolve this equation with a simple Euler scheme, taking time steps empirically chosen to be $h = t_0/128$ [t_0 being the time scale defined in Eq. (11)], and imposing periodic boundary conditions. The choice of the time step is very critical because of the very different and variable time scales involved in this kind of simulation.

We tested grids of N^2 sites, with $N = 128$, 256, and 512. It is convenient to employ larger grids, not only because of less granularity in the observed density, but also because it is possible to achieve sufficient statistics with fewer runs for ensemble. We have made about 20 runs for each ensemble, which means that the dispersions of field and defect density are in the $\sim 3\%$ level. We choose the net parameters $a_x = a_y = \xi_0/2$, in order to resolve adequately the shape of the defects, which are expected to have a final size $d \approx \xi_0$.

The initial conditions were set in two different ways. We obtain a thermal distribution of modes, employing expression (14) as the dispersion of a Gaussian distribution of the mode amplitudes, with $\xi = \xi_0/2$, that is a temperature equal to five times T_c. The cutoff was set up at the maximum radius in k space, i.e., $k_{\max} = 2\pi/\xi_0$. The results are cutoff independent, in any case, due to the rapid decay of the short-wavelength modes in the first steps of the quench. At the end of the quench, these modes grow again in order to define the final shape of the defects. Following Ref. [24], we tested $\mu = 10^{-2}, 10^{-3}, 10^{-4}$, and 10^{-5}.

Alternatively, we started the field by choosing uniformly at random the phase of the order parameter between 0 and 2π, and its modulus between 0 and $\rho = 10^{-4}$ (in one set of simulations) or between 0 and $\rho = 10^{-6}$ (in another set). As expected, the results obtained are mostly independent of how the initial conditions are set [27].

C. Numerical experiments

The presence of topological defects (or candidate ones) in the field $\Delta(\mathbf{x})$ can be determined from the fact that for any closed curve C we have

$$\oint_C d\mathbf{x} \cdot \boldsymbol{\nabla} \theta(\mathbf{x}) = 2\pi n_C, \tag{21}$$

where $\Delta(\mathbf{x}) = \rho(\mathbf{x}) \exp[i\theta(\mathbf{x})]$, and n_C is the total topological charge of the defects inside the curve. By candidate topological defects we mean those who have a net circulation of the phase, but not the equilibrium profile. That is, we have the phase defect, but the modulus is still evolving.

The presence of a vortex can be observed through expression (21). Numerically, we will sum the shortest difference of the phase of the order parameter field along the lines between nodes of the grid surrounding each plaquette. Let us call

$$s(\alpha,\beta) = \beta - \alpha, \quad if(s > \pi) s = s - 2\pi, \quad if(s < -\pi) s = s + 2\pi. \tag{22}$$

So, four neighbor sites i,j,k, and l; oriented counterclockwise, will yield

$$v = \frac{1}{2\pi} (s(\theta^j, \theta^i) + s(\theta^k, \theta^j) + s(\theta^l, \theta^k) + s(\theta^i, \theta^l)) = \pm 1, 0. \tag{23}$$

This device can only measure vorticity $|v| \leqslant 1$. So we cannot detect a pair vortex-antivortex laying in a single plaquette, nor vortexes with greater vorticity. But this is enough, given the mutual annihilation of very close vortexes and the almost absolute absence of higher vorticity, which can be seen in the representation of the phase of the order parameter field. By the way, periodic boundary conditions provide a test of the accuracy of the observation, because the net vorticity must vanish. Higher sensitivity devices can be implemented considering higher plaquettes, which means more surrounding sites.

The reciprocal representation of the field is obtained through the usual fast Fourier transform [28]. In two dimensions this gives a discrete representation of $\tilde{\Delta}(\mathbf{k})$ at sites $\mathbf{k}$

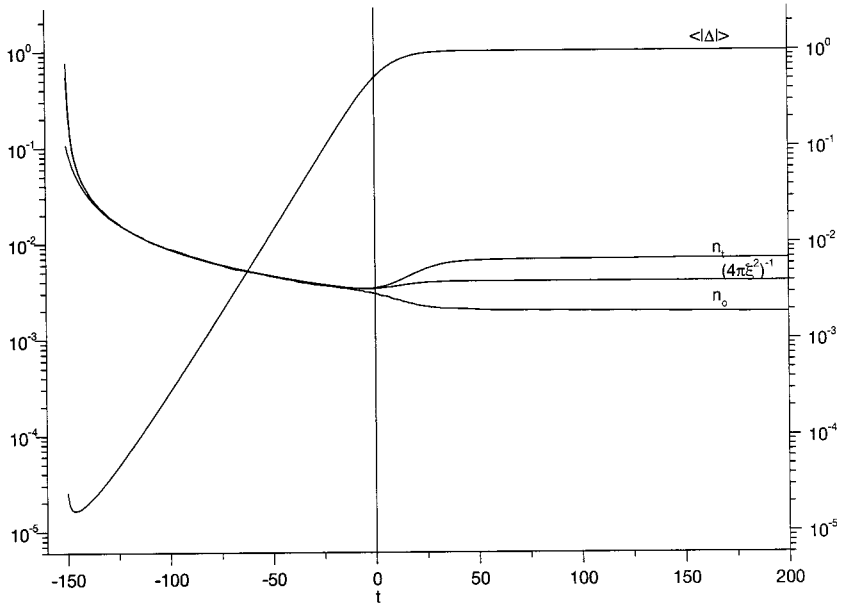

FIG. 1. Ensemble average of the absolute value of the order parameter field $\langle|\Delta|\rangle$, the HML prediction n_t for the defect density, the magnitude $1/(4\pi\xi^2)$ [where ξ is the correlation length measured from a fit of the long-wavelength part of the correlation function, as in Eq. (26)], and the observed defect density n_o, all as functions of time. This run corresponds to $\mu=10^{-4}$ and $T=2$. Initially ξ differs from both the predicted and observed densities, but the rise of the gauge field smears out this difference. While the graph of $\langle|\Delta|\rangle$ changes concavity at $t=0$, this is not easily appreciated due to the distortion caused by the linear-logarithmic scales. The same curve is plotted in linear-linear scales in Fig. 3.

$=(n,m)(2\pi/Na)$ with $n,m=-N/2,\ldots,(N/2)-1$, and a is the net parameter supposed equal in both directions. With our discretization, $\mathbf{k}=(n,m)(4\pi/N\xi_0)$, and the domain of the reciprocal representation embodies the circle $k<2\pi/\xi_0$, as well as a number of higher modes.

The various mean values of the field can be obtained easily in each time step, since the space and ensemble average commute. On the other hand, the power spectrum requires saving each run for further processing.

In order to try to measure the correlation length, we consider the k^2 dependence of the ensemble dispersion g_k^2 of the amplitude of the k_{th} mode:

$$g_k^2=\langle|\tilde{\Delta}(\mathbf{k})|^2\rangle. \tag{24}$$

For a thermal distribution this is a straight line,

$$\frac{1}{g_k^2}=\frac{k^2+\xi^{-2}}{\mu}. \tag{25}$$

We can estimate $\mu/g_k\to\xi^{-2}$ when $k^2\to 0$, through a linear fit of the ensemble media of the spectra. This is a rough estimate, but gives a qualitative description of the behavior of the correlation length.

A better determination of the correlation length can be obtained from the out of equilibrium distribution of modes [19] (see below). At long wavelengths $k^2<\xi^{-2}$,

$$g_k^2\approx h e^{-\xi^2 k^2}. \tag{26}$$

This factor can also be measured from a linear fit, and the system quickly reaches this regime.

IV. RESULTS

A. Anatomy of a quench

Figure 1 shows a typical evolution of a quench. We have plotted the ensemble average of the absolute value of the order parameter field $\langle|\Delta|\rangle$, the HML prediction n_t for the defect density, the magnitude $1/(4\pi\xi^2)$ [where ξ is the correlation length measured form a fit of the long-wavelength part of the correlation function, as in Eq. (26)], and the observed defect density n_o, all as functions of time. This run corresponds to $\mu=10^{-4}$ and $T=2$. We have chosen $t=0$ as the point where the second derivative of the order parameter changes sign.

Figure 2 shows $\langle|\Delta|\rangle$, n_t, and n_o for all six ensembles tested. The time scales are shifted in order to make all the inflection points of $\langle|\Delta|\rangle$ coincide. We can see that the behavior of each ensemble is essentially the same.

Once the simulation begins, the gauge field (initially null) adjusts itself in order to follow the order parameter field, reacting back on it. This is what can be expected from the very different time scales involved in Eqs. (19) and (20), and it appears in the graph as the initial decay of the order parameter field. The observed discrepancy between predicted and observed defect densities is quickly smeared out by the evolution of the field. Actually neither of them is reliable this early in the simulation, since the prescribed thermal distribution has too much power at short wavelengths, which can be eliminated with a cutoff. Furthermore the algorithm to identify defects is blind to higher vorticity monopoles. Both errors are quickly self-corrected, however, as the density of defects decays and the distribution of modes becomes a Gaussian function, as in Eq. (26). This Gaussianity should not be confused with that of the ensemble, but just refers to the shape of $g(k)^2$.

The first stage of the quench (once the transient is over) is characterized by the exponential grow of the order parameter field, which can be parametrized empirically as $\langle|\Delta|\rangle=2e^{0.159t-1}\approx 2e^{(t/2\pi)-1}$ (the dashed line in Fig. 2), where t is the synchronized time. While this is to be expected from the growth of the spinodal instability, it must be observed that we are already beyond the linear regime at this stage. This is the regime where the HML prediction is essentially exact. The ensemble probability density of the field is clearly Gaussian, as can be tested by the ratio $\langle|\Delta|^4\rangle\langle|\Delta|^2\rangle^{-2}$. In fact, for a Gaussian ensemble, considering only diagonal terms of the correlation, we have $\langle|\Delta|^4\rangle=2\langle|\Delta|^2\rangle^2$. We have plotted this ratio vs time, in Fig. 3, together with the ratio n_t/n_o and $\langle|\Delta|\rangle$. The plot represents the average of these

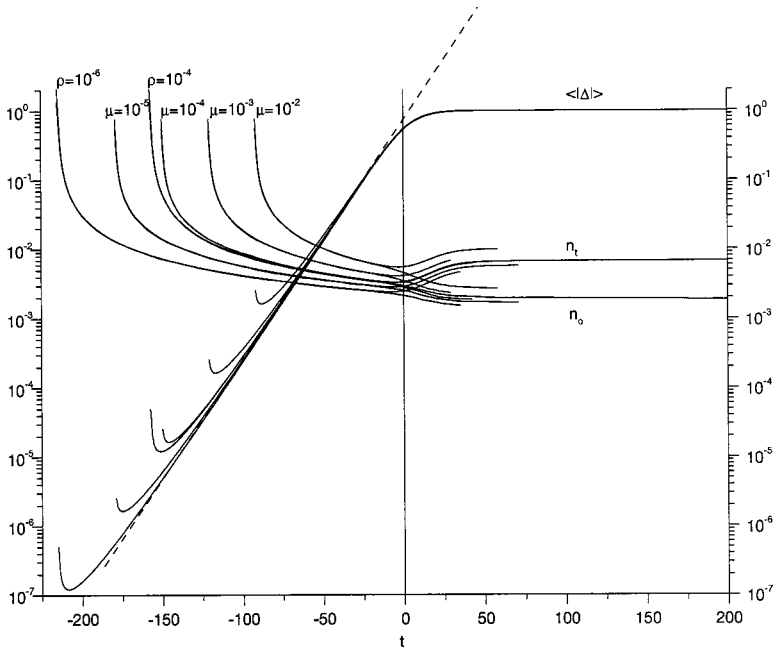

FIG. 2. $\langle|\Delta|\rangle$, n_t, and n_o for all six ensembles. All ensembles has been synchronized at the inflection points of the curves $\langle|\Delta|\rangle$. Also represented are the defect densities predicted and observed.

quantities over all six ensembles; the dotted lines around the first two represent the dispersion between ensembles. The dashed lines around the plot of the order parameter represent the empirical fit to an exponential, and the tangent at the inflection point. When the growth of the average order parameter ceases to be exponential (around $t\sim-50$; see Fig. 4), we enter a transition regime where first the Gaussianity of the ensemble, and then the HML prediction cease to hold.

In the final stage, from $t\sim25$ on, the approach to the equilibrium value is also exponential, as can be appreciated in Fig. 4, where we have plotted the time derivative of $\langle|\Delta|\rangle$, with linear-logarithmic scales. In this final stage, the exponential behavior of the field is $\propto 1-e^{-0.134t}$, and the topological defects have attained almost their stable profiles (see below).

We can see that, as long as the ensemble is Gaussian, the HML prediction is exact for all practical purposes. Around $t\sim-30$, both Gaussianity and the exponential growth of the order parameter break down; however, the HML estimate is still a good approximation until later times, $t\sim-10$.

B. Evolution of the structure function

The two main regimes in the evolution of the quench, the early one dominated by the growth of the order parameter and the late one dominated by the evolution of the defect network, are also clearly seen in the evolution of the structure function, namely, the Fourier transform of the equal time order parameter correlation function (for the structure function in systems with global symmetry, see Ref. [29]).

At early times and long wavelengths, the order parameter and the gauge field are essentially decoupled. Under this approximation, the dynamical equation [Eq. (12)] becomes

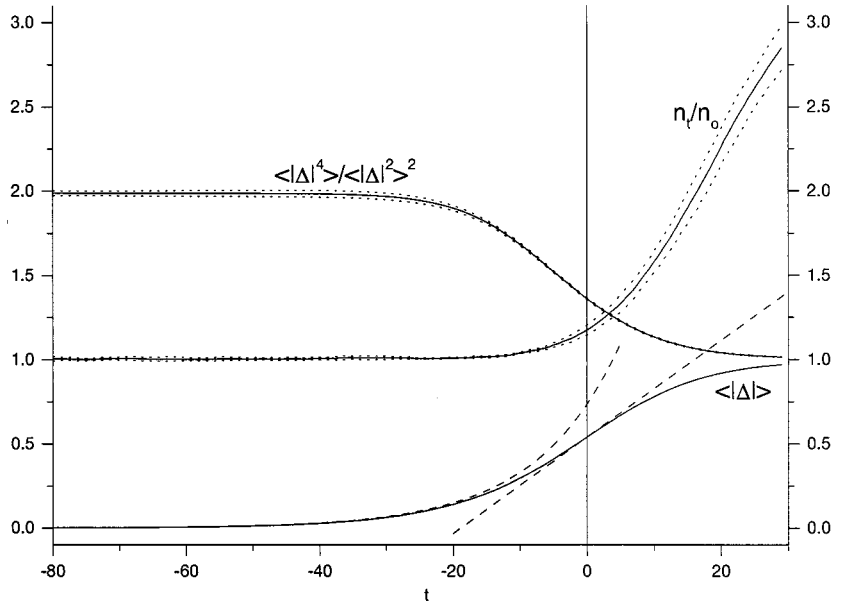

FIG. 3. $\langle|\Delta|^4\rangle\langle|\Delta|^2\rangle^{-2}$, as a function of time, together with the ratio n_t/n_o and $\langle|\Delta|\rangle$. The plot represents the average of these quantities over all six ensembles; the dotted lines around the first two represent the dispersion between ensembles. The dashed lines around the plot of the order parameter represent the empirical fit to an exponential, and the tangent at the inflection point. The ratios show that the predicted and observed defect densities agree very well even when the field distribution ceases to be Gaussian.

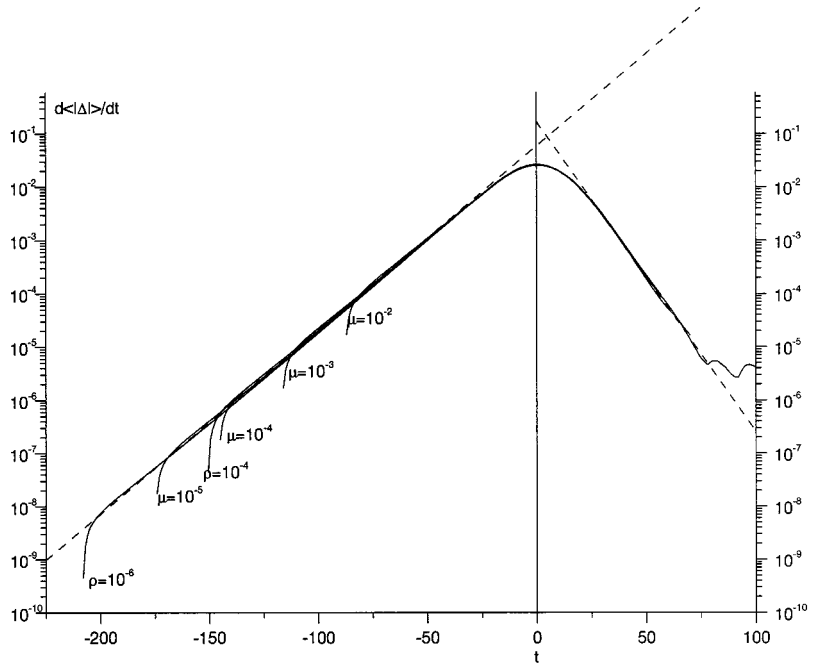

FIG. 4. Time derivative of $\langle|\Delta|\rangle$; there is no symmetry at all between both sides of the inflection point.

$$\frac{\partial}{\partial t}\Delta = \frac{1}{12}[\nabla^2\Delta + \Delta]. \tag{27}$$

Assuming that each mode has a random initial phase, the theoretical prediction for the structure function at early times and long wavelengths is

$$g_k^2 \sim \exp\left\{\left(\frac{t}{6}\right)[1-k^2]\right\}. \tag{28}$$

In particular, the correlation length, determined from the scaling condition $g_k^2 \sim f(\xi k)$, grows as $\sqrt{t}$. In Fig. 5 we plot the correlation length squared as a function of time for each ensemble; the result clearly agree with expectations. In this regime calculation (5) reduces to $n_t \approx 1/4\pi\xi^2$, which, as we have seen, agrees very well with the observed density.

For later times and wavelengths shorter than the average defect separation, the structure function is dominated by the profile of an isolated defect. The Abrikosov-Gorkov vortex centrated at the origin is given by

$$\Delta \sim (1-e^{-r/r_1})e^{i\theta}, \tag{29}$$

where r_1 is the characteristic size of the defect. The Fourier transform of this shape gives

$$\tilde{\Delta}_k \sim \frac{2\pi}{k^2}[1-(1+r_1^{-2}k^{-2})^{-3/2}]e^{-i\mathbf{k}\cdot\mathbf{x}_0}, \tag{30}$$

with x_0 the position of the defect. Considering short wavelengths, as compared to the average defect separation, we obtain

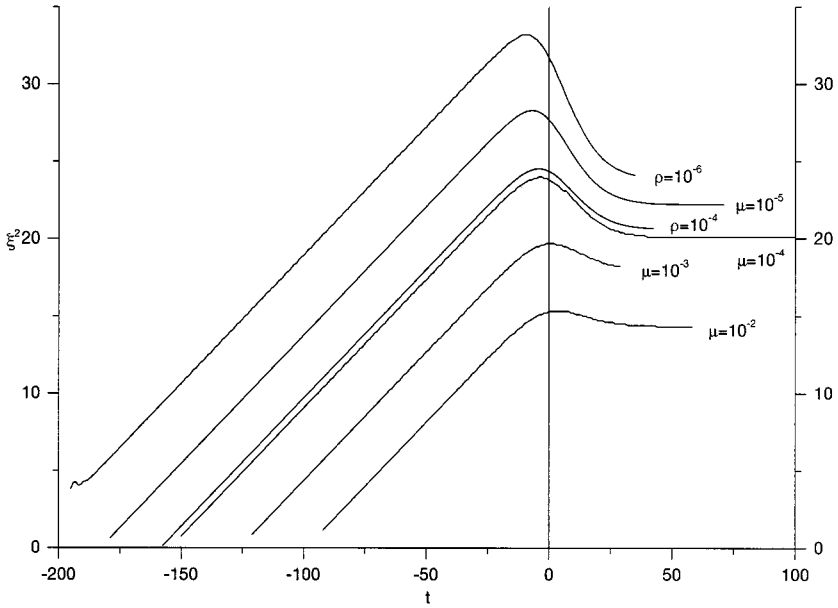

FIG. 5. Correlation length squared as a function of time for each ensemble. The initial linear growth of ξ^2 stops simultaneously with the slow down in the growth of the order parameter field. These curves agree very well when represented in simulation time, rather than shifting time to make the inflection points coincide.

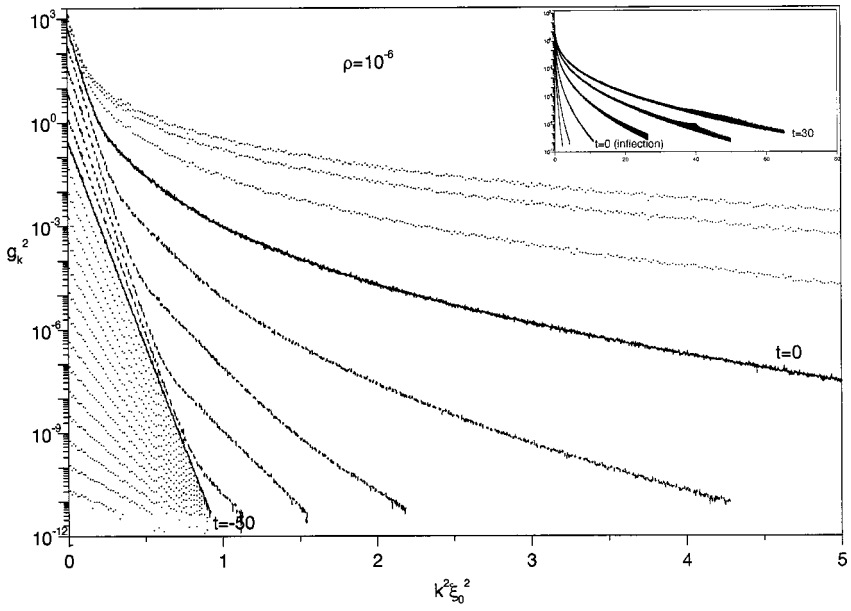

FIG. 6. Power spectra measured for the ensemble $\rho=10^{-6}$ at equally spaced different times, as a function of $\xi_0^2k^2$, for random initial conditions and $\rho=10^{-6}$; the vertical scale is logarithmic. The first bold curve corresponds to the time at which the spectrum leaves the behavior $g_k^2 \approx he^{-\xi^2(k^2-1)}$. The second corresponds to the inflection time. The inset shows the growth of short-wavelength modes needed for the final shape of the defects.

$$g_k^2 \sim |\tilde{\Delta}_k|^2 n_o, \tag{31}$$

where n_o is the observed density of defects. By construction, a grid cannot support singularities like that at the origin in Eq. (29), but the power law characteristic of Eq. (31) is the kind of spectrum we hope to find in the final regime of the quench.

Figure 6 displays the evolution of the structure function (plotted every ten time units) as a function of $\xi_0^2k^2$, for random initial conditions and $\rho=10^{-6}$; the vertical scale is logarithmic. The early plots clearly display the Gaussian behavior predicted by Eq. (28). After $t=-50$ (bold line) the short-wavelength modes begin to grow beyond the early time prediction. The second bold line represents the structure function at $t\sim 0$, that is, the beginning of the late time regime. The inset shows the same plot, for a wider range in wave number. Figure 7 shows the same for the thermal initial conditions, and $\mu=10^{-4}$. The same behavior is obtained, and it is remarkable that the value of g_k^2 for $k\xi_0=1$ remains constant over the early time regime.

In Fig. 8, we contrast three of the structure functions shown in Fig. 7 (corresponding to times $t=50$, 70, and 340) with the structure function of an isolated defect, as given by Eqs. (30) and (31), given by the solid line. For visual effect, we have overestimated slightly the value of n_o in Eq. (31). We have set $r_1=1$, as predicted by theory.

C. Epoch of defect formation

Candidate defects exist from the very beginning of the quench, as can be detected from the phase of the order parameter field, and predicted by the HML formula. It is the development of a well-defined vortex and the pattern of supercurrents around it which makes the system leave the Gaussian distribution. The exponential growth slows down as soon as the modes stop behaving almost independently ($t\sim -30$). The formation of the shape of the vortex itself is also starting at this time.

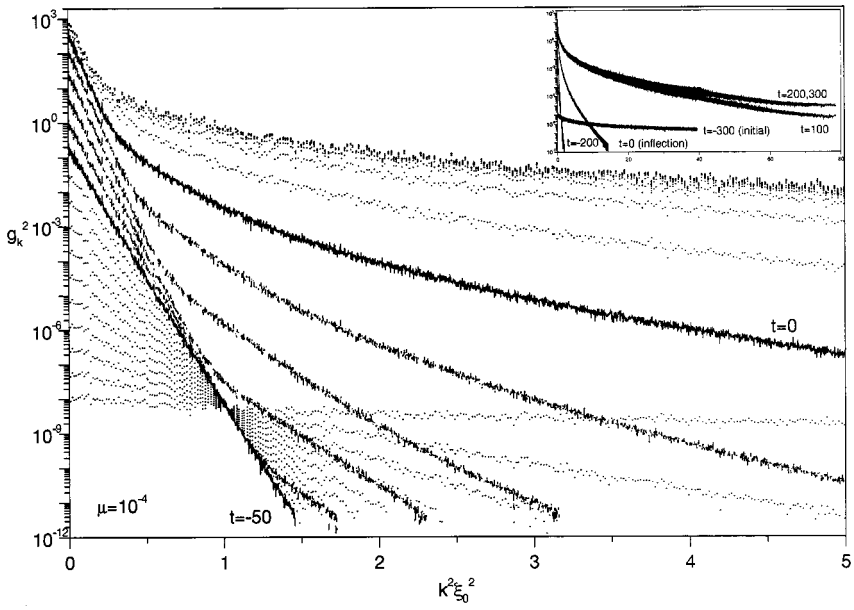

FIG. 7. Power spectra for the ensemble $\mu=10^{-4}$. Note the initial decay of the short-wavelength modes. At late times these modes grow again, and for this ensemble the shape of the vortex almost reaches its equilibrium form.

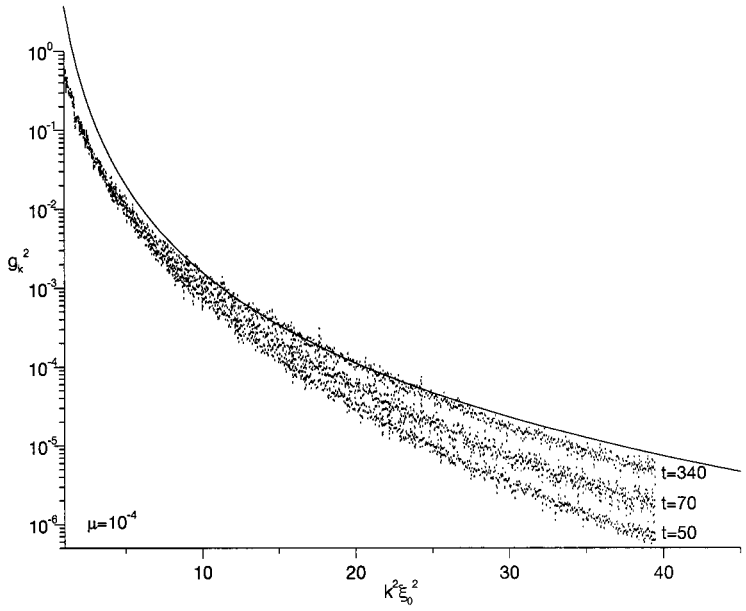

FIG. 8. Detail of the previous figure. The solid curve correspond to $\gamma[x^{-1}(1-(1+x)^{-3/2})]^2$ [see Eq. (30)], and the factor γ is approximately equal to the final density of defects. Only the modes corresponding to the maximum circle in reciprocal space are depicted ($k^2\xi_0^2<4\pi^2$).

We may follow the formation of the vortexes through the evolution of the ''kinetic'' free energy [30]

$$K=\frac{1}{V}\int d^2x\,|(-i\nabla-\mathbf{A})\Delta|^2$$

$$=\frac{1}{V}\int d^2x\,\{|\nabla\rho|^2+\rho^2|\nabla\theta-\mathbf{A}|^2\}, \qquad (32)$$

where $\Delta=\rho e^{i\theta}$, and the last term corresponds to the supercurrents. Initially K is very low, and starts building up with the steeping of the field gradients around the candidate defects. When the defect attains its final shape, both $\nabla\rho$ and the current die out outside the core, but there is a core contribution left, and so K reaches a final value which is proportional to the defect density. The subsequent evolution of K simply follows the slow decay of the defect density due to defect-defect annihilation.

Figure 9 shows the ensemble average of K/n_o (also averaged over the six ensembles considered) as a function of time. For comparison purposes we also show $\gamma\langle|\Delta|\rangle$ (dashed line), where $\gamma=4.82$ is the asymptotic value of K/n_o. At time $t\sim 70$ the final shape and current has been reached, and the tiny fluctuations are due to transients corresponding to vortex annihilation. A remarkable implication of Fig. 9 is that defect formation occurs at a relatively well defined epoch, from $t\sim -30$ to 40.

D. Final remarks

This paper attempts to answer the question of how reliable are estimates of the defect density based on the approximation of Gaussian ensembles as applied to nonlinear phase transitions. To this effect, we have independently measured the Gaussian prediction and the actual defect density as a function of time after an instantaneous quench to zero temperature in a two-dimensional superconductor. The evolution of the quench goes through three stages: an initial one domi-

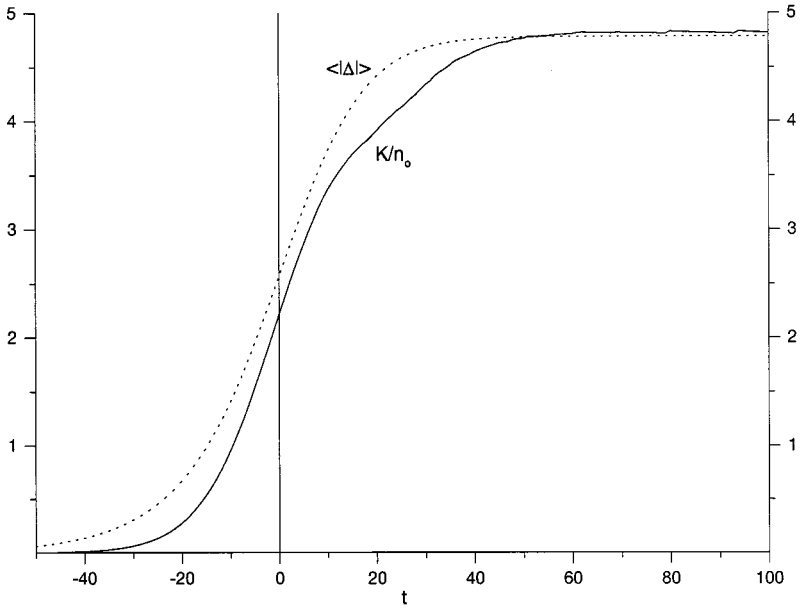

FIG. 9. Ensemble average of K/n_o (also averaged over the six ensembles considered) as a function of time. For comparison purposes we also show $\gamma\langle|\Delta|\rangle$ (dashed line), where $\gamma=4.82$ is the asymptotic value of K/n_o, showing the final average between the kinetic term and the defect density.

nated by the unfolding of the spinodal instability, a final one dominated by defect-defect interactions, and a transitional stage when most defects are actually formed.

We find that the Gaussian estimate is essentially exact over the early regime, and continues to be accurate almost to the end of the epoch of defect formation. This moment in time is marked by the jump in the ''kinetic'' energy K [see Eq. (32)]; it is also the time when the order parameter reaches about half of its equilibrium value. While the Gaussian estimate itself is not reliable beyond this point, it is still a valid tool to fix the initial conditions of the defect network, whose subsequent evolution must be investigated by other means (like those in this paper, or in Ref. [8]).

These results confirm theoretical expectations, but it is nevertheless satisfactory to have solid numerical proof of formerly theoretical conjectures. The very detailed view of the process of defect formation which is afforded by our simulations should also be valuable in investigating more subtle processes, such as preheating during the nonequilibrium phase transition [31] or instabilities due to strong field effects [32]. Also, by doing a more complete simulation, where we could also control the quench rate, it ought to be possible to investigate Zurek and co-workers conjecture about the scaling of the defect density with the quench rate [10,11,14]. Finally, it is of interest to perform simulations in regions of parameter space approaching actual experimental contexts. We continue our research in these manyfold directions.

ACKNOWLEDGMENTS

It is a pleasure to acknowledge many conversations with Bei-lok Hu, Steve Ramsey, and Greg Stephens. This work was partially supported by UBA, CONICET, Fundacion Antorchas, and FOMEC.

[1] B. Halperin, in *Physics of Defects*, edited by R. Balian, M. Kleman, and J. P. Poirier (North-Holland, New York, 1981).
[2] F. Liu and G. F. Mazenko, Phys. Rev. B **44**, 9185 (1991); **45**, 6989 (1992); **46**, 5963 (1992).
[3] G. Karra and R. J. Rivers, e-print hep-ph/9603413.
[4] C. Nash and S. Sen, *Topology and Geometry for Physicist* (Academic Press, London, 1983).
[5] P. M. Chaikin and T. C. Lubensky, *Principles of Condensed Matter Physics* (Cambridge University Press, New York, 1995).
[6] S. Coleman, *Aspects of Symmetry* (Cambridge University Press, New York, 1988).
[7] K. Huang, *Quarks, Leptons and Gauge Fields* (World Scientific, Singapore, 1992).
[8] A. Vilenkin and E. P. S. Shellard, *Strings and Other Topological Defects* (Cambridge University Press, Cambridge, 1994).
[9] T. W. B. Kibble, J. Phys. A **9**, 1387 (1976).
[10] W. H. Zurek, Nature (London) **317**, 505 (1985); Phys. Rep. **276**, 178 (1996); P. Laguna and W. H. Zurek, Phys. Rev. Lett. **78**, 2519 (1997); and e-print cond-mat/9705141; J. R. Anglin and W. H. Zurek, e-print quant-ph/9804035; P. Laguna and W. H. Zurek, Phys. Rev. D **58**, 85 021 (1998); N. D. Antunes, L. M. A. Bettencourt, and W. Zurek, e-print hep-ph/9811462.
[11] A. Yates and W. H. Zurek, Phys. Rev. Lett. **80**, 5477 (1998).
[12] I. Chuang, R. Durrer, N. Turok, and B. Yurkee, Science **251**, 1336 (1991;); M. J. Bowick, L. Chandar, E. A. Schiff, and A. M. Srivastava, *ibid.* **263**, 943 (1994).
[13] P. C. Hendry *et al.*, Nature (London) **368**, 315 (1994); C. Bauerle *et al.*, *ibid.* **382**, 332 (1995); V. M. Ruutu *et al.*, *ibid.* **382**, 334 (1996); Phys. Rev. Lett. **80**, 1465 (1998).
[14] G. Karra and R. J. Rivers, e-print hep-ph/9804206; E. Moro and G. Lythe, e-print cond-mat/9811032; E. Kavoussanaki and R. J. Rivers, e-print cond-mat/9901348.
[15] M. Bowick and A. Momen, e-print hep-ph/9803284; N. Goldenfeld, in *Formation and Interactions of Topological Defects*, edited by A. -C. Davis and R. Brandenberger (Plenum Press, New York, 1995) (preprint, hep-ph/9411380); N. D. Antunes and L. M. A. Bettencourt, Phys. Rev. D **55**, 925 (1997); J. Dziarmaga, e-print cond-mat/9803185; G. Vincent, N. D. Antunes, and M. Hindmarsh, Phys. Rev. Lett. **80**, 2277 (1998); N. D. Antunes, L. M. A. Bettencourt, and A. Yates, e-print hep-ph/9901391 v2.
[16] G. J. Stephens, E. A. Calzetta, B. L. Hu, and S. A. Ramsey, Phys. Rev. D **59**, 45 009 (1999).
[17] A. J. Gill and R. J. Rivers, Phys. Rev. D **51**, 6949 (1995); G. Karra and R. J. Rivers, Phys. Lett. B **414**, 28 (1997).
[18] E. Calzetta, Ann. Phys. (N.Y.) **190**, 32 (1989).
[19] D. Boyanovsky, Da-Shin Lee, and A. Singh, Phys. Rev. D **48**, 800 (1993).
[20] L. P. Gorkov and G. M. Éliashberg, Zh. Éksp. Teor. Fiz. **54**, 612 (1968) [Sov. Phys. JETP **27**, 328 (1968)].
[21] Michael Tinkham, *Introduction to Superconductivity*, 2nd ed. (McGraw-Hill, New York, 1996).
[22] A. Abrikosov, L. Gorkov, and I. Dzyaloshinsky, *Methods of Quantum Field Theory in Statistical Physics* (Dover, New York, 1963).
[23] C. R. Hu and R. S. Thompson, Phys. Rev. B **6**, 110 (1972); A. Schmid, Phys. Rev. **180**, 527 (1969).
[24] R. Kato, Y. Enomoto, and S. Maekawa, Phys. Rev. B **44**, 6916 (1991); **47**, 8016 (1993); Physica C **227**, 347 (1994); **263**, 21 (1996).
[25] F. J. Alexander, S. Habib, and A. Kovner, Phys. Rev. E **48**, 4284 (1993).
[26] See the discussion on the relevance (in the sense of renormalization group theory) of the final temperature in Ref. [27].
[27] A. J. Bray, Adv. Phys. **43**, 357 (1994).
[28] W. H. Press *et al.*, *Numerical Recipes*, 2nd ed. (Cambridge University Press, Cambridge, 1992).
[29] G. Mazenko and R. Wickham, e-print cond-mat/9607152; M. Mondello and N. Goldenfeld, Phys. Rev. A **45**, 657 (1992).
[30] E. M. Lifshitz and L. P. Pitaevskii, *Statistical Physics Part 2: Theory of the Condensed State* (Pergamon Press, Oxford, 1980).
[31] S. Khlebnikov, e-print hep-ph/9708313v2.
[32] D. Boyanovsky, F. Cooper, H. de Vega, and P. Sodano, e-print hep-ph/9802277.